UDC 532. 528 : 621. 224. 2

CAVITATION CHARACTERISTICS OF FORCED VORTEX CORE IN THE FLOW OF THE FRANCIS TURBINE

Takashi Kubota

Hiroshi Matsui

Kawasaki Factory

I. INTRODUCTION

In recent years, there has been a tendency to use higher specific speeds for hydraulic turbine and pump-turbine. The popularity of underground hydro-storage plants has prompted to select the lower installation height of hydraulic turbine and pump-turbine and because of large variations in the tail water level, aeration to the draft tube has become difficult. In addition, the influence of the suction head on the vibration characteristics during partial load operation presents a problem.

In the runner outlet of Francis turbines, the whirl gradually increases at points further away from the best efficiency point and therefore the forced vortex core occurs in the center of the upper draft tube. As the pressure in the vortex core is small, the forced vortex core cavitates itself when the sigma decreases and a large cavity can be formed in the center of the core. The forced vortex core becomes especially large during partial load operation, and the cavity in the center makes a periodic eccentric movement in the upper draft tube. In this way, the well-known surge phenomena appear. However, definite measurement results of the changes which occur in the forced vortex core and the hydraulic surge when there are changes in sigma have rarely been reported up to the present. Therefore, Fuji Electric first worked with many model turbines in its hydraulic laboratory and studied the cavitation characteristics of the forced vortex core during operation at partial, loads. These characteristics are described in this article.

On the other hand when cavitation tests were performed at overloads on model turbines with low specific speeds, it was found that there was no cavitation on the surface of the runner vanes but in spite of this there was a gradual decrease in turbine efficiency η from test conditions with a large sigma as test sigma decreased.

One special characteristic of this phenomenon was that whenever it occurred, there was always a large forced vortex core in the runner outlet. So far, the relations between the critical sigma σ_c unrelated to the runner vane cavitation and the forced vortex core have not been pointed out up to the present. Therefore, the cavitation characteristics of the forced vortex core during overload operation is also discussed.

II. CAVITATION CHARACTERISTICS OF FORCED VORTEX CORE DURING PARTIAL LOAD OPERATION

1. Experimental Equipments and Measuring Methods

The high head cavitation test stand in the hydraulic laboratory of Fuji Electric was used and experiments concerning the relation between suction head H_S and the hydro-surge at partial load operation were performed using model Francis turbines with $n_s=80$ to 300 m/kW. *Fig. 1* shows a typical model turbine of $n_s=150$/kW undergoing a test.

In the models, the upper part of the draft tube was made of transparent plexiglass so that the behavior of the forced vortex core inside the tube could be observed visually. The hydro-surging phenomenon was recognized by visual observation. Pressure transducers with strain gauges were attached to the walls of the spiral case inlet and the draft tube inlet, and the hydraulic pressure fluctuations were recorded on an oscillograph. By reading out the amplitude A_S (total amplitude) and the periods, the surge intensity was measured. The static pressure H_C at the center of the forced vortex core was measured by inserting a cylindrical probe with two holes into the center of the upper draft tube.

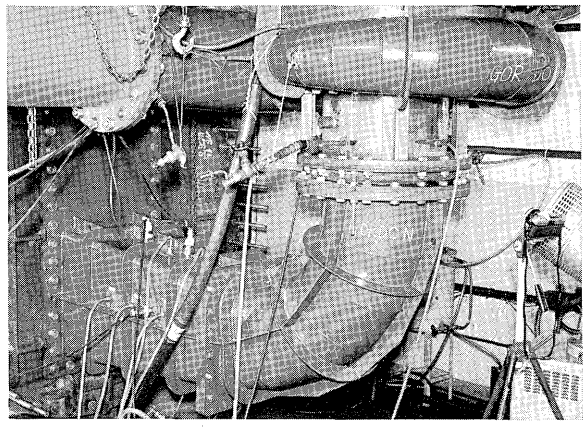

Fig. 1 Typical model turbine on test ($n_s=150$ m-kW)

Under constant test head conditions, the distributor was fixed at the gate opening at which surge occurs, the suction head of the turbine was changed (i.e. the test sigma was changed), and the behavior of the forced vortex core, the hydraulic pressure fluctuations, the pressure in the center of the draft tube, etc. were measured.

2. Cavitation Characteristics of the Forced Vortex Core

Hydraulic surge phenomena during partial load operation generally occur in the 40 to 80% range of the best gate opening a_{0opt} at the optiumum efficiency point for the rated head. It is generally most strong at around 60% opening.

Therefore, the gate opening was first set at 60% a_{0opt}, and the hydraulic pressure fluctuation As at the inner wall of the upper draft tube and the static pressure H_C at the center of the forced vortex core when the suction head H_S was changed were measured. Typical results of these measurements

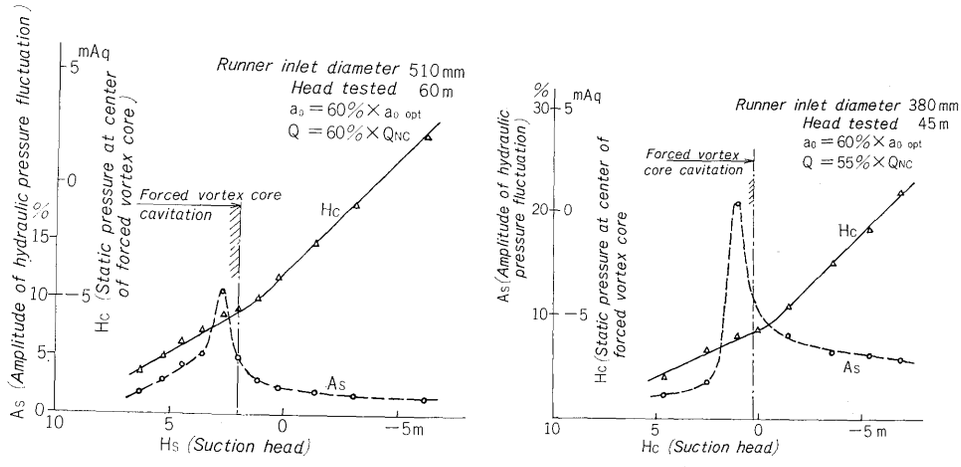

(a) n_s=100 m-kW (b) n_s=220 m-kW

Fig. 2 Amplitude of pressure surge A_s and static pressure of forced vortex core Hc versus suction head H_s

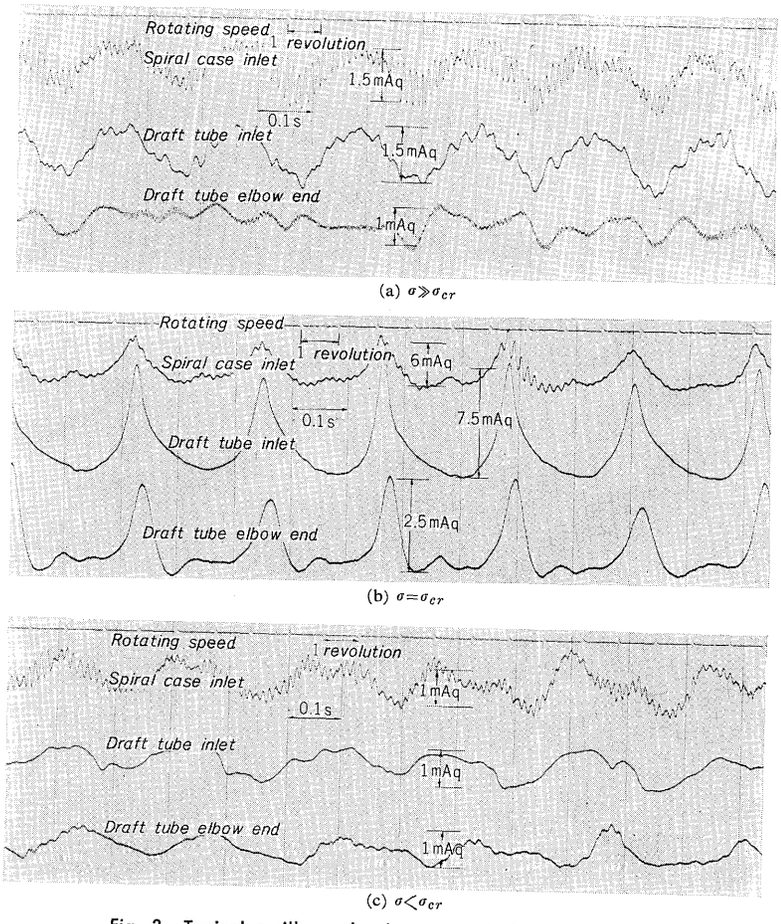

(a) $\sigma \gg \sigma_{cr}$

(b) $\sigma = \sigma_{cr}$

(c) $\sigma < \sigma_{cr}$

Fig. 3 Typical oscillographs showing variation of pressure surge for various suction head (n_s 150 m-kW)

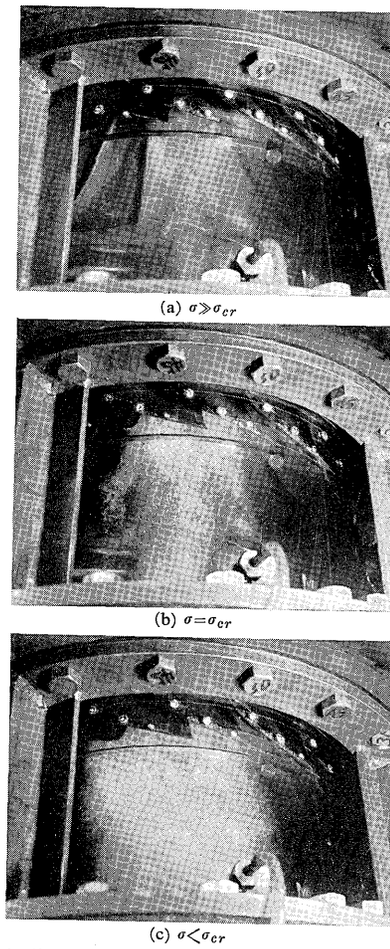

(a) $\sigma \gg \sigma_{cr}$

(b) $\sigma = \sigma_{cr}$

(c) $\sigma < \sigma_{cr}$

Fig. 4 Typical photos showing variation of forced vortex core for various suction head

are shown in *Fig. 2* (a) for a turbine of $n_s=100$ m/kW, and in *Fig. 2* (b) for a turbine of $n_s=220$ m/kW. The Q_{NC} in the figure is the discharge at which there is no whirl in the runner outlet (no whirl flow), and A_S is the total amplitude of the hydraulic pressure fluctuation expressed as a percentage of the test head. *Fig. 3* shows typical oscillographs of hydraulic pressure fluctuation for a turbine of $n_s=150$ m/kw. *Fig. 4* shows photographs of the runner outlet corresponding to the oscillographs.

When the suction head is small (i.e. sigma is large), the forced vortex core in the upper draft tube can not be observed visually since the cavitation phenomenon does not occur. Surge noise and hydraulic pressure fluctuations are also relatively small (refer to *Figs. 3* (a) and *4* (a)).

When the suction head is increased, and the static pressure H_C at the center of the vortex core decreases, a unclear shape appears since cavitation starts in the forced vortex core. At the start of this condition, the linearity of H_C in respect to H_S starts to break down, and the hydraulic pressure fluctuations increase sharply. When cavitation progresses and the forced vortex core can be observed clearly to fluctuate eccentrically, the maximum fluctuation is reached (refer to *Figs. 3* (b) and *4* (b)). The maximum amplitude of fluctuation is shown as $A_{S\max}$. If H_C at this time, is expressed as H_{Ccr} then $H_{Ccr}=-6$ to -7 m.

The waveform of the hydraulic pressure fluctuation is a sinusoidal curve when sigma is large (*Fig. 3* (a)), but at the time of the maximum hydraulic pressure fluctuation, it becomes a sharp pulse curve (*Fig. 3* (b)). The frequency of the fluctuation is not related to H_S and is approximately one time for every four rotations of the runner. The phase is almost the same for all the measuring locations (spiral case inlet, upper draft tube), and it suggests the cause of turbine vibration.

When H_S increases further, the amounts of dissolved air and floating air in water which collects in the forced vortex core increase and a condition arises just as if the upper draft tube was aerated. The forced vortex core then breaks down, the eccentric fluctuating movement is greatly reduced, the hydraulic pressure fluctuations are minimized, the fluctuation waveform breaks down and the periods become vague (refer to *Figs. 3* (c) and *4* (c)).

3. Operation Conditions at which Hydraulic Pressure Fluctuations Reach a Maximum

As was described above, experiments were carried out concerning the forced vortex core cavitation characteristics by altering various combinations of the gate opening and unit speed n_{11}. *Fig. 5* shows the typical example of the maximum amplitude of hydraulic pressure fluctuations $A_{S\max}$ and the critical static pressure at the center of the foreced vortex core H_{Ccr} versus the ratio of the flow to the no whirl flow Q/Q_{NC} for the respective combinations. From these graphs, it was confirmed that the $A_{S\max}$ maximum at $Q/Q_{NC}\fallingdotseq 0.55$ for turbines of any specific speed n_s. In the end, under operating conditions where the combination of gate opening and unit speed was such that the turbine flow was approximately 55% of the no whirl flow, the hydraulic pressure fluctuations are the maximum at the suction head where the static pressure at the center of the forced vortex core becomes -6 to -7 m-Aq as gauge pressure and large vibrations appear in the

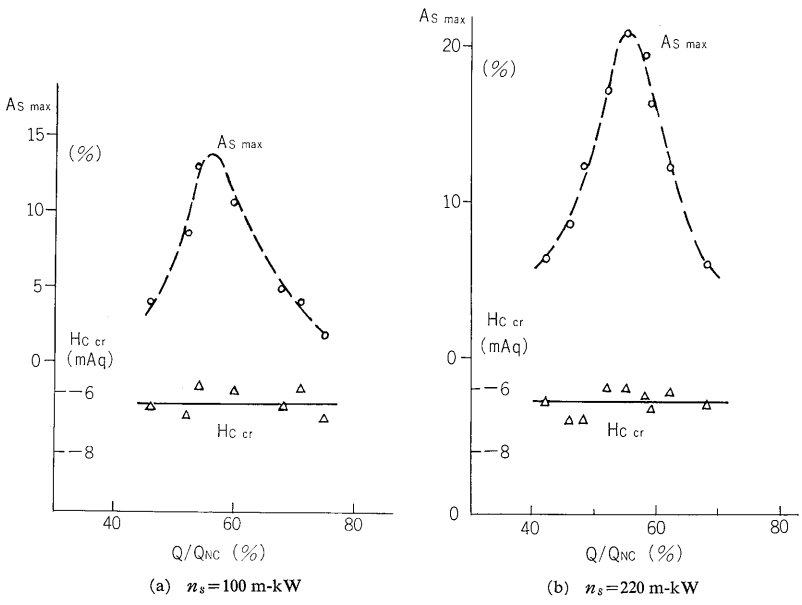

(a) $n_s=100$ m-kW (b) $n_s=220$ m-kW

Fig. 5 Maximum amplitude of pressure surge $A_{S\max}$ and critical static pressure of vortex core H_{Ccr} versus every operating condition (Q/Q_{NC})

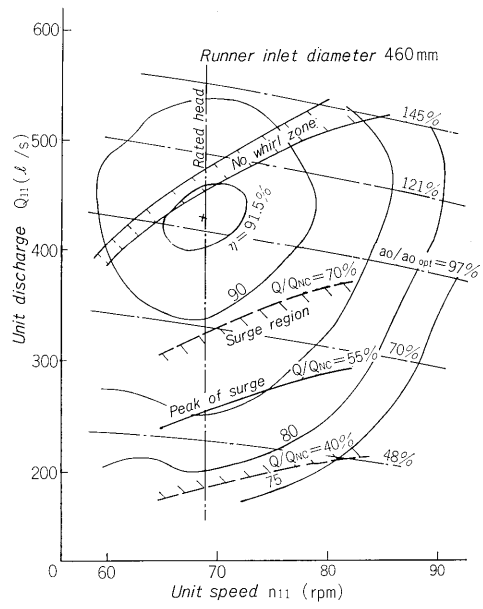

Fig. 6 Pressure surge region on the unit characteristic curve of Francis turbine

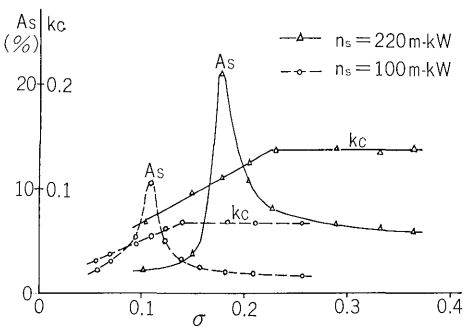

Fig. 7 Non-dimensional expression of Fig. 2 (Static pressure coefficient of vortex core k_c versus sigma)

turbine. The diameter of the forced vortex core when the surge is maximum is 40 to 50% of the inlet diameter of the draft tube and it can be observed visually that the eccentric fluctuations are very large.

Fig. 6 shows the typical region of surging due to the forced vortex core on the unit characteristics curve (shell curve) of the Francis turbine. The surge region is about $Q/Q_{NC}=40$ to 70% irrespective of the specific speed n_s.

4. Cavitation Similitude of the Forced Vortex Core

As was described above, it is clear that the surge phenomena in hydraulic turbines are closely related to the cavitation characteristics of the forced vortex core. However, it is necessary to elucidate a similitude for cavitation of the forced vortex core in order to estimate the prototype turbine conditions from the model test results.

Fig. 7 shows a non-dimentional representation of the relation between H_C and H_S as shown in *Fig. 2* with the static pressure coefficient designating the ratio of the pressure drop (from the total pressure H_S to the pressure H_C) to the head tested, i.e. $k_c=(-H_S-H_C)/H$, versus sigma on the abscissa. In the range of large sigma, the static pressure coefficient k_c at the center of the core is a flat straight line but when the forced vortex core begins cavitation, the core static pressure coefficient begins to change and the hydraulic pressure fluctuation increases rapidly.

However, the value of k_c which shows the core static pressure drop per unit head (flat line in *Fig. 7*) is affected by the whirl intensity at the runner outlet. Therefore, the value of k_c can be influenced by the differences in the shape of runner vanes and/or draft tube and in the unit speed tested, because these differences change the whirl intensity at runner outlet. In addition, the value of the critical static pressure coefficient when the hydraulic pressure fluctuations are a maximum, $k_{ccr}=(-H_{Scr}-H_{Ccr})/H$, becomes not always constant and therefore, it is not appropriate to use this k_c for the similitude.

However, since the critical static pressure in the core H_{Ccr} is almost constant as was described previously, the critical static pressure in the core as an absolute pressure $H_C{}^*{}_{cr}$ ($H_C{}^*{}_{cr}=H_a+H_{Ccr}$) can be used in place of the vapor pressure of water H_v in the Thoma's cavitation coefficient $\sigma=(H_a-H_v-H_S)/H$ and a new coefficient of λ can be defined as follows:

$$\lambda=\frac{H_a-H_C{}^*{}_{cr}-H_S}{H} \quad \cdots\cdots\cdots\cdots\cdots (1)$$

If this new coefficient λ is the same between model and prototype, it is possible to consider the state of the core will become similar. Actually, by changing the range of test heads from 25 to 65 m in some model turbines, it was confirmed that the similitude was established by λ.

However, the value of the critical static pressure in the core $H_C{}^*{}_{cr}$ was not always 3 to 4 m (−7 to −6 m as gauge pressure) and had a considerable influence on the whirl intensity at the runner outlet. The factors which have a large effect on the value of $H_C{}^*{}_{cr}$ are as follows:

1) Runner: the intensity of the whirl at the runner outlet is changed in accordance with the shape of the runner. Especially when the runner outlet diameter is large, the discharge angle of the runner vane and the discharge vent becomes small and the whirl becomes intense. Therefore, $H_C{}^*{}_{cr}$ has a tendency to decrease.

2) Draft tube: when the divergent angle of the draft tube inlet and the diffusion ratio of the cross-sectional area from the elbow are small, a strong vortex tends to be formed so that it is also likely that the value of $H_C{}^*{}_{cr}$ will drop. The vortex is difficult to diffuse when the cross-sectional shape from the elbow is almost circular and the $H_C{}^*{}_{cr}$ tends to decrease.

Therefore, when there is a combination of a runner with a large outlet diameter and a circular draft tube of small divergence, the critical static pressure in the core $H_C{}^*{}_{cr}$ can be almost equal to the vapor pressure of water, H_v, and dereases to about 0.5 m-Aq ($H_{Ccr}=-9.8$ m as gauge pressure).

When there is the model test result available as mentioned above, from the critical static pressure in the core $H_C{}^*{}_{cr}$ obtained in the model tests and

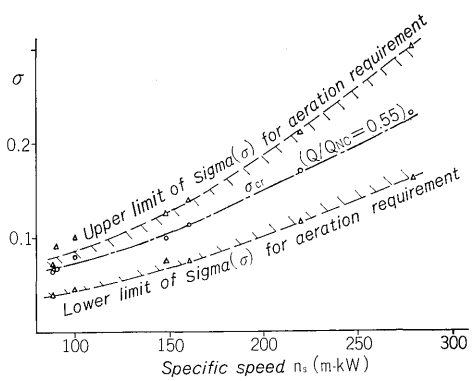

Fig. 8 Critical sigma σ_{cr} versus specific speed n_s

the lambda of equation (1), the following is obtained :

$$H_{S\lambda}=H_a-H_C{}^*{}_{cr}-\lambda H \quad \cdots\cdots\cdots\cdots (2)$$

where,

$H_{S\lambda}$: suction head of prototype converted by λ in meter

H_a : atmospheric pressure in m-Aq

$H_C{}^*{}_{cr}$: critical static pressure in the vortex core (on the assumption that the values of the prototype and model are equal) in meter

λ : cavitation coefficient according to equation (1) obtained from the model tested

H : net head in meter

Therefore, conversion to a prototype can be achieved. However, since the value of the critical static pressure in the core is less constant compared with the vapor pressure of water H_v as was described previously, it is necessary to use data prepared from the previous sigma instead of lambda in the preliminary projection and when model tests are not performed. *Fig. 8* shows the critical sigma σ_{cr} at the $Q/Q_{NC}=0{\cdot}55$ where the hydraulic pressure fluctuations are maximum from the model tests and the range of sigma where the surge is so strong that aeration is required. In this case :

$$H_{S\sigma}=H_a-H_v-\sigma\cdot H \quad \cdots\cdots\cdots\cdots (3)$$

When ΔH_S is designated as the deviation of $H_{S\sigma}$ from $H_{S\lambda}$ by equation (2), then from equations (2) and (3) :

$$\Delta H_S\equiv H_{S\lambda}-H_{S\sigma}$$
$$=(h_C{}^*{}_{cr}-H_v)\frac{H}{h}-(H_{Ccr}-H_v)$$

where the small letters are for the model and the capital letters are for the prototype. If it is assumed that $h_C{}^*{}_{cr}=H_C{}^*{}_{cr}$, then :

$$\Delta H_S=(H_C{}^*{}_{cr}-H_v)\left(\frac{H}{h}-1\right) \quad \cdots\cdots\cdots\cdots (4)$$

For example, if the critical static pressure in the core $H_C{}^*{}_{cr}=3.4$ m, the vapor pressure of water $H_v=0.4$ m and the ratio of the head of the prototype to that of the model is $H/h=2$, then from equation (4), ΔH_S becomes 3 m. Therefore, when the value of $H_C{}^*{}_{cr}$ is rather high and the model head is small in respect to the actual head, it is possible that the estimate value of the suction head H_S calculated from sigma is too low (i.e. the tail water level too high). It is necessary to take this into consideration.

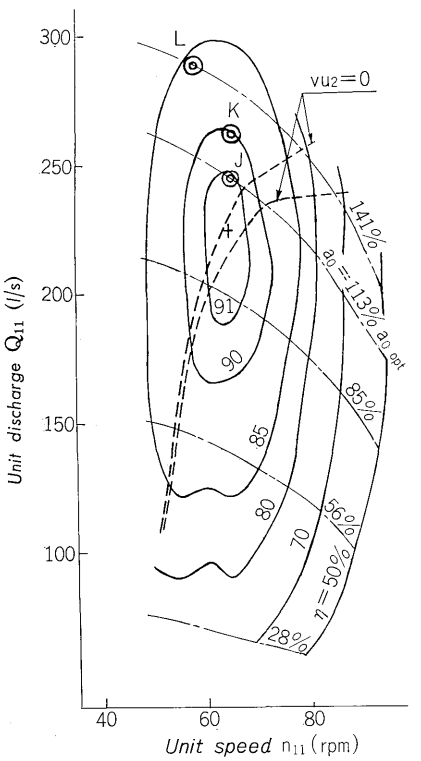

Fig. 9 Test points on the unit characteristic curve of Francis turbine (n_s=100 m-kW)

III. CAVITATION CHARACTERISTICS OF THE FORCED VORTEX CORE OPERATING AT OVERLOADS

1. General Cavitation Characteristics Operating at Full Load

When the Francis turbine is operated at rated head, the maximum load acting on the runner vane is naturally atfull load. The static pressure on the low pressure surface of the runner vane (especially near the runner band at the outlet) decreases and is very likely that cavitation will occur. A typical example of the cavitation characteristics at full load (poin J in *Fig. 9*) is shown in *Fig. 10* (a). This example shows the results of a cavitation test performed at a head of 60 m on a model turbine of $n_s=100$ m-kW and runner diameter $d_1=510$ mm with a gate opening of 113% (full opening) at the point of maximum efficiency. In the unit charac-

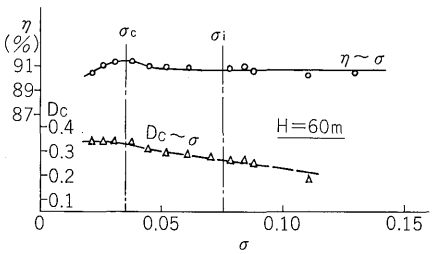

(a) Full load (Point-J on Fig. 9)

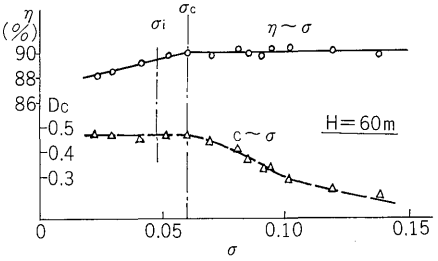

(b) Over load (Point-K on Fig. 9)

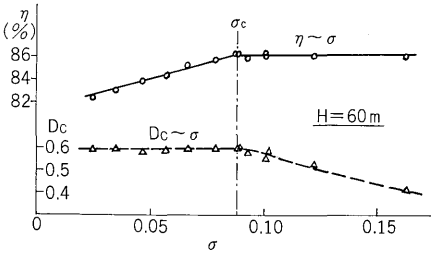

(c) Extream over load (Point-L on Fig. 9)

Fig. 10 Cavitation characteristics of Francis turbine (n_s=100 m-kW)

teristics cureves (shell curves) for this turbine shown in *Fig. 9*, the one-dot chain lines show the unit discharge $Q_{11}=q/(d_1^2\cdot\sqrt{h})$ versus the unit speed $n_{11}=n\cdot d_1/\sqrt{h}$ for the respective gate opening, and the solid lines show the efficiency contour lines. The broken lines show the zone of no whirl at the runner outlet ($v_{u2}=0$). When the test head was held constant, the runner outlet pressure was decreased and the sigma tested (horizontal axis in *Fig. 10* (a)) reached to σ_i, cavitation was incipient on the low pressure surface of the runner vane outlet near the band and when the test sigma was even smaller, cavitation increased. Once a large degree of cavitation was achieved, turbine efficiency η generally started to decrease (critical sigma σ_c).

2. Special Cavitation Characteristics during Operation at Overloads

The above are the ordinary cavitation characteristics at full load operation. At overload operation, the incipient sigma of cavitation σ_i as well as the critical sigma at which the turbine efficiency starts to drop σ_c both generally become large. However when the degree of overload is high, the critical sigma of the efficiency drop σ_c can become larger than the incipient sigma σ_i. This is true in the case of 127% gate opening in the above example (point K in *Fig. 9*). The cavitation characteristic curve in this case is shown in *Fig. 10* (b). When sigma is large, there is no cavitation at all on the runner vane but the turbine efficiency starts to drop. After the sigma decreases further, cavitation becomes incipient on the runner vane. In such cases, there is almost no growth of cavitation on the runner vane even when the sigma is reduced further. When the overload conditions increase (point L in *Fig. 9* when the unit speed drops to 89% of the rated speed and the guide vane opening increases to 141%), the critical sigma of the efficiency drop σ_c increases still more and contrarily the runner vane cavitation does not occur even at the minimum sigma available for the test (refer to *Fig. 10* (c)).

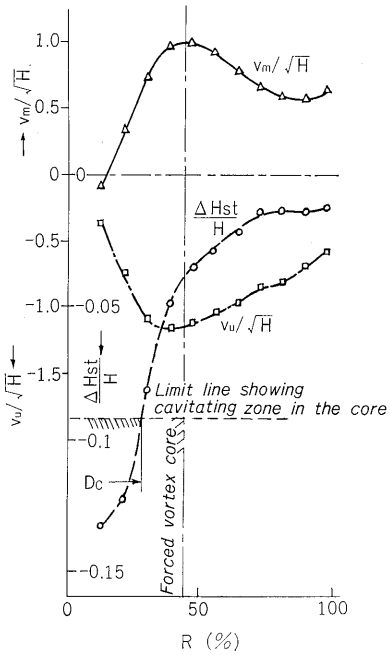

Fig. 11 Flow distribution in upper draft-tube (Point-K on Fig. 9)

3. Cavitation Characteristics of Forced Vortex Core

From the above test results, it is apparent that the critical sigma of efficiency drop during operation at overloads is quite different from that during operation at full loads, and it has no relation with runner vane cavitation. When this phenomenon occurs, the main characteristic is the existence of strong foreced vortex core which grows at the runner outlet as was described in the introduction. This can be considered at the reason why points K and L in *Fig. 9* are far away from the no whirl zone (broken line zone). This can be seen in the cavitation characteristics of the foreced vortex core.

When the sigma at points K and L is reduced, it is observed visually that the cavitating zone (visible portion) in the forced vortex core becomes larger. By inserting a measuring rod into the upper draft tube which is made of transparent plexiglass, the diameter of the cavitating zone in the vortex core d_C was measured. The lower part of *Fig. 10* shows the changes of the ratio of this diameter d_c to the runner outlet diameter d_2, $D_C=d_c/d_2$, for various values of sigma. *Figs. 10* (b) and (c) shows very clearly the relation between the turbine efficiency η and the cavitation diameter D_C of the vortex core. In other words, even when the test sigma decreases, turbine efficiency does not change so far as the cavitating zone in the vortex core continues to grow and D_C continues to increase. However, when the cavitating zone in the forced vortex core is completed to grow (i.e. the whole of the vortex core reaches the cavitation state) and D_C becomes constant, it is evident that the efficiency starts to decrease simultaneously.

4. Flow Distribution at Runner Outlet

Fig. 11 shows the velocity and static pressure distribution in the upper draft tube at the point K in *Fig. 9* to give some indication of the flow distribution at the runner outlet under overload conditions when the above phenomena occur. The measurements were made by inserting a cylindrical probe in the same position as the measuring rod to measure the cavitation diameter of the vortex core. The abscissa in *Fig. 11* shows the radial location in the draft tube ($R=100\%$ at inner wall of tube). In this figure, v_m is the meridional component of the flow velocity, v_u is the peripheral component of flow velocity (negative sign designates the reverse direction to the runner rotation), and ΔH_{ST} is the difference between the static pressure of flow H_{ST} and the

suction head H_S expressed as total pressure,

$$\Delta H_{ST} = H_{ST} - (-H_S).$$

From this figure, it is evident that a decrease in the test sigma causes the cavitation limit line shown by the broken line to be raised. Therefore, the cavitating zone in the vortex core steadily increases, and D_C becomes larger. However, since the radial gradient of the static pressure H_{ST} in the forced vortex core is large, there is almost no effect on the region of free vortex flow outside of the forced vortex flow. However, after the whole region of the forced vortex core is in the cavitation state, the static pressure no longer decreases linearly in the region of free vortex flow even when sigma is decreased further, and therefore the substantial effective head is decreased and the turbine efficiency drops. Even when the test sigma is less than the incipient sigma σ_i in *Fig. 10* (b) runner vane cavitation does not grow because the static pressure in the region of free vortex flow is not decreased as much as the decrease of sigma. Also in the case of *Fig. 10* (c), it can be understood why the static pressure in the region of free vortex flow can not decrease to the incipient pressure.

From the above, the abnormal phenomenon in which the efficiency gradually drops from a high sigma which appears during overload operation in low specific speed turbines at low unit speed n_{11} (higher head), has no relation to runner vane cavitation and can be considered to be due to the cavitation in the forced vortex core which grows up strongly. It is also necessary to consider the effect of the test head in relation to the forced vortex core cavitation phenomenon during overload operation. However, in the test region where the test head was altered in the model turbine between 40 and 80 m, the similitude for sigma was achieved. In the future, the work will be continued to study the similitude for critical static pressure in the vortex core.

IV. CONCLUSION

Experimental research has been carried out using a series of model turbines concerning the cavitation characteristics of the forced vortex core created by the whirl which occurs at the runner outlet of the Francis turbine. Some considerations on the following two relations have been given :

(1) the relation between the forced vortex core cavitation characteristics and the hydraulic pressure fluctuations during partial load operation.
(2) the relation between the forced vortex core cavitation characteristics and the abnormal efficiency drop during overload operation.

It is hoped that this work will contribute to invetigations concerning the installation height of new types of hydraulic turbines in the future.